Biosensors and Bioelectronics 24 (2009) 1424–1430

Contents lists available at ScienceDirect

Biosensors and Bioelectronics

journal homepage: www.elsevier.com/locate/bios

Polyazetidine-based immobilization of redox proteins for electron-transfer-based biosensors

Marco Frasconi, Gabriele Favero, Massimo Di Fusco, Franco Mazzei*

Università degli Studi di Roma "La Sapienza", Dipartimento di Chimica e Tecnologie del Farmaco, Piazzale Aldo Moro 5, 00185 Rome, Italy

ARTICLE INFO

Article history:
Received 4 June 2008
Received in revised form 28 July 2008
Accepted 11 August 2008
Available online 22 August 2008

Keywords:
Immobilization
Electrochemical biosensor
Electron transfer

ABSTRACT

A highly stable functional composite film was prepared using polyazetidine prepolymer (PAP) with peroxidase from horseradish (HRP) and/or glucose oxidase (GOx). The good permeability of the PAP layer to classical electrochemical mediators, as evaluated by the determination of the diffusion coefficient of different redox molecules, is of great importance in view of the use of PAP as an immobilizing agent in second-generation biosensor development.

Cyclic voltammetry of the HRP–PAP layer on a glassy carbon electrode (GCE) showed a pair of stable and quasi-reversible peaks for the HRP–$Fe^{(III)}/Fe^{(II)}$ redox couple at about −370 mV vs. Ag/AgCl electrode in pH 6.5 phosphate buffer. The electrochemical reaction of HRP entrapped in the PAP film exhibited a surface-controlled electrode process. This film and the successive modifications (HRP–PAP self-assembled monolayer (SAM) modified Au electrode) were used as a biological catalyst (hydrogen peroxide transducers) for glucose biosensors, after coupling to GOx. Both HRP/GOx–PAP and HRP/GOx–PAP SAM third generation biosensors were prepared and characterized.

The use of PAP as immobilizing agent offers a biocompatible micro-environment for confining the enzyme and foreshadows the great potentiality of this immobilizing agent not only in theoretical studies on protein direct electron transfer but also from an applications point of view in the development of second- and third-generation biosensors.

1. Introduction

One of the most important aspects that have to be taken into account in the development of electron-transfer-based biosensors is represented by the redox proteins immobilization on the electrode surface. An ideal immobilization procedure should ensure the stable presence of the proteins at the electrode surface, maintaining their electrocatalytic properties and, at the same time, allowing a good accessibility to the target analyte, redox mediators and an efficient communication with the electrode surface (Armstrong and Wilson, 2000; Katz and Willner, 2004; Wang, 2008). For these reasons the protein immobilization procedure and its improvement are of paramount importance in order to enhance biosensor performance. This is particularly important in the development of third generation biosensors (Shan et al., 2007; Zhang et al., 2004). These biosensors are characterized by several advantages over the traditional electrochemical biosensors: indeed, the possibility of having direct electron transfer between the protein and the electrode surface enables biosensors to be constructed without the use of redox mediators which are characterized by higher selectivity, because they can operate in a potential window closer to the redox potential of the enzyme leading to a lower sensitivity towards possible interfering reactions (Gorton et al., 1999). Despite these advantages, direct electrical communication between redox proteins and electrode supports is uncommon as it is often hindered by the inaccessibility of the protein redox centre, which thus limits the development of this type of biosensor (Lu et al., 2006). The considerable progress made in this field has evidenced that the modification of electrodes using appropriate support may provide a favorable micro-environment for the protein to exchange its electron directly with the underlying electrode and thus affords a new opportunity for the detailed study of enzyme electrochemistry (De Groot et al., 2007). In the last few years several immobilization procedures suitable for studying direct electron transfer have been developed (Lu et al., 2007; Zhang et al., 2007; Wang et al., 2003). Most of them are characterized by both advantages and drawbacks, the greatest of which generally consist of (i) the difficulty to ensure an adequate protein mobility in order to correctly orientate its redox centre, and thus to achieve a better electron transfer with the electrode surface and (ii) the possible denaturation of the proteins when they are directly adsorbed on to the electrode, leading to the loss of any electrochemical activity (De Groot et al., 2005).

* Corresponding author.
E-mail address: franco.mazzei@uniroma1.it (F. Mazzei).

0956-5663/$ – see front matter © 2008 Elsevier B.V. All rights reserved.
doi:10.1016/j.bios.2008.08.017

In the past we used polyazetidine prepolymer (PAP) to fabricate first generation biosensors (Mascini and Mazzei, 1987; Botrè et al., 1992; Mazzei et al., 1996, 2004). In the present work we describe the employment of PAP as immobilizing agent for redox proteins on electrodes with a view to characterizing their electrocatalytic properties in both direct and mediated electron transfer phenomena. In particular, we describe a simple method for developing an enzymatic electrode by immobilizing two of the most important redox enzymes: peroxidase from horseradish (HRP) and glucose oxidase (GOx), in a polyazetidine layer on different electrode surfaces. Studies performed on the direct electrochemistry of immobilized HRP indicate that it displays enhanced direct electron transfer and excellent electrocatalytical performance for its principal substrate: H_2O_2 (Zhuo et al., 2006). Moreover, the HRP-based enzymatic electrodes obtained were tested as hydrogen peroxide transducers for building glucose biosensors. One further investigated aspect is the construction of mediated electron-transfer-based biosensors employing GOx immobilized on the electrode surface in the presence of a redox mediator, either free in solution or immobilized in the enzymatic layer. In view of the possible use of PAP as immobilizing agent for second-generation biosensor fabrication, the polymer permeability to redox mediator was also evaluated. To this end, the diffusion coefficient of different redox mediators using the same electrode surface before and after PAP deposition was determined.

2. Experimental

2.1. Materials

Horseradish peroxidase (HRP) type VI-A (EC 1.11.1.7, MW 42.1 kDa), glucose oxidase (GOx) type VII from *Aspergillus niger* (EC 1.1.3.4, MW 160 kDa) potassium ferricyanide $K_3[Fe(CN)_6]$ (FCN), 2-2′-azino-bis(3-ethylbenzothiazoline-6-sulfonic acid) diammonium salt (ABTS) and ferrocene monocarboxylic acid (FCA) were obtained from Sigma (Sigma–Aldrich, USA); mercaptopropionic acid (MPA) >99% and 4-aminothiophenol (NTP) >97%, from Aldrich (Sigma–Aldrich, USA), while Polyazetidine prepolymer® was donated by Hercules, Inc., Wilmington (DE, USA).

Sodium phosphate, hydrogen peroxide, glucose and other chemicals were all of analytical grade. High purity deionized water (resistance: 18.2 MΩ × cm at 25 °C; TOC: <10 μg/L) obtained from a Millipore Direct-Q 3 UV system (Millipore, France) was used throughout the experiments.

2.2. Methods

2.2.1. Electrochemical measurements

Electrochemical measurements were carried out in aqueous solution in the presence of 0.1 M KCl as supporting electrolyte for diffusion coefficient determination or in phosphate buffer 0.1 M, pH 6.5 (PB) for all the other measurements. The measuring solution was deoxygenated by purging N_2 for at least 20 min and kept under a constant stream of N_2 throughout measurement; electrochemical experiments were carried out in a thermostated glass cell using a μ-Autolab (EcoChemie, The Netherlands) and a typical three-electrode configuration. An $Ag/AgCl/KCl_{sat}$ (198 mV vs. NHE) was used as reference electrode (Cat. 6.0726.100, Metrohm, Switzerland) and a glassy carbon rod as counter electrode (Cat. 6.1241.020, Metrohm, Switzerland). Different working electrodes were employed, in particular: for the determination of the diffusion coefficient, a Pt microdisk (PtM) diameter 20 μm embedded in glass (Amel, Italy) was used; on the other hand, for the electron transfer studies and to fabricate different sensors and biosensors, different classical working electrodes were investigated: a glassy carbon electrode (GCE), diameter 3 mm (Cat. 6.1204.300, Metrohm, Switzerland) and a polycrystalline gold electrode (AuE) diameter 3 mm (Cat. 6.1204.320, Metrohm, Switzerland). Alternatively, experiments were performed also by using graphite screen printed electrodes (SPE) (Cat. AC1.W4.R1, BVT, Czech Republic) previously polished electrochemically by polarization at −2 and +2 V for 20 min.

The active electrochemical surface of classical working and screen printed electrodes was determined by chronocoulometry and was found to be 0.0746 cm^2 for GCE and 0.00798 cm^2 for SPE, respectively. The Pt microdisk electrode radius was determined before every measurement.

2.2.2. Diffusion coefficient determination

The measurement of diffusion coefficients of redox species is usually carried out using the Randles–Sevcik equation, which requires that the compound's concentration be known. This is not a problem when the species are free in solution; conversely, when a redox compound is entrapped or immobilized to some extent, its concentration in the embedding layer is generally different to the bulk concentration; moreover, it is often difficult and sometimes impossible to specify (Petrovic et al., 2000). In the present work we used the normalized form of the Cottrell equation (Denuault et al., 1991) which allows the diffusion coefficients of the selected redox compounds to be calculated without having to know their concentrations in the PAP layer:

$$i_d = \frac{\sqrt{\pi} nF \sqrt{D_0} Cr^2}{\sqrt{t}} + 4nFD_0Cr$$

where i_d is the diffusion current, $i_{d,ss}$ the steady-state current, D_0 the diffusion coefficient, t is the time elapsing after the application of an appropriate potential step and r is the radius of the microdisk electrode.

This equation can be used to plot $i_d/i_{d,ss}$ vs. $t^{-1/2}$, thus obtaining a straight line whose intercept is unity and whose slope is α:

$$\alpha = \frac{\sqrt{\pi r}}{4\sqrt{D_0}}$$

From the α value calculated by plot linearization, it is possible to obtain D_0 provided that the radius r is known: the latter can be evaluated by performing a similar experiment using a redox species of known diffusion coefficient.

In practice, a platinum microdisk (PtM), 20 μm diameter, was used as working electrode; before every experiment the electrode's radius was calculated from the steady-state current using a $K_4Fe(CN)_6$ solution as reported in literature (Adams, 1969). The electrode was first polished on alumina powder of different size (0.3 and 0.05 μm) and then ultrasonically cleaned in water for about 5 min. The PAP-coated electrode was prepared by spreading 2 μL of a PAP solution containing 1.5×10^{-5} M bovine albumin serum (BSA) over the electrode surface and allowing it to dry overnight. BSA in the PAP layer allows the presence of a generic protein in the membrane to be simulated while embedding an enzyme would have caused interference by reacting with the redox mediators considered.

All the measurements were the average of at least 10 replicated measurements.

2.2.3. Immobilization procedure using PAP

The immobilization procedure is based on the use of polyazetidine which performs both a chemical immobilization and a physical entrapment. This is possible thanks to the features characterizing the polyazetidine prepolymer.

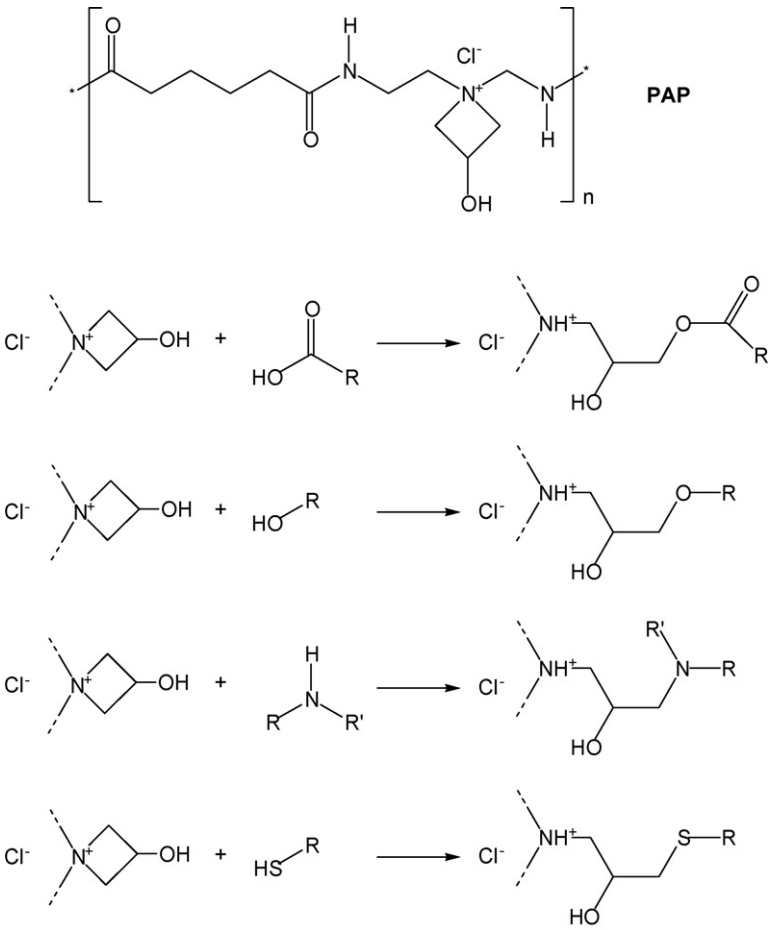

Scheme 1. PAP structure and typical reactions.

PAP acts as a cross-linking agent as it is able to react with several different organic moieties (thiolic, oxydril, carboxyl, and amino groups), thus increasing the likelihood of chemical bonds being created with the enzyme and thereby enhancing immobilization efficiency (see Scheme 1).

This scheme of possible reactions involving PAP and some of the most important organic moieties emerges from the characterization performed by Hercules, Inc., and was confirmed by us in several previously published papers (Mascini and Mazzei, 1987; Botrè et al., 1992; Mazzei et al., 1996, 2004).

The HRP–PAP sensors described below were obtained by casting on the electrode surface a suitable amount (10 μL for GCE and AuE) of an HRP 1.5×10^{-5} M solution in polyazetidine prepolymer and allowing it to dry at room temperature overnight.

In the case of HRP–PAP SAM-based sensors, a gold electrode (AuE) was previously mechanically polished using diamond paste and alumina and then sonicated for 30 s in order to remove all alumina residues. Then, AuE was also electrochemically polished by performing several cyclic voltammetric scans in H_2SO_4 0.5 M in the range 0–1.5 V vs. $Ag/AgCl/KCl_{sat}$ until a constant profile was obtained. Finally, AuE was covered with a self-assembled monolayer (SAM) of mercaptopropionic acid or 4-aminothiophenol (NTP), obtained by immersion in a millimolar solution of the selected modifying agent overnight. After SAM formation the electrode was treated with PAP as described above.

Glucose oxidase (GOx) second-generation biosensors were prepared by casting on the electrode surface 10 μL of 1.5×10^{-5} M GOx solution in PAP; alternatively, for third generation biosensor preparation, 10 μL of a mixture containing both HRP and GOx (in the ratio 1:1) dissolved in PAP were spread onto a bare or SAM covered electrode surface, accordingly.

Once formed, the polyazetidine membrane (PAP) embedding enzyme(s) was equilibrated for 10 min in measuring buffer before starting the electrochemical experiment.

3. Results and discussion

The PAP was studied as immobilizing agent for redox proteins in the preparation of both second- and third-generation biosensors based on HRP and/or GOx.

As far as the development of second-generation biosensors is concerned, the permeability of the PAP layer to different mediators in solution was determined and the performance of GOx–PAP-mediator-based biosensors employing different electrode materials was evaluated.

Furthermore, with regard to the use of PAP for third generation biosensor development, the electron transfer kinetic and the bioelectrochemical properties of HRP-based biosensors using different electrode materials (either bare or SAM covered electrodes) were studied. Then, the HRP–PAP and HRP–PAP SAM biosensors thus obtained were also employed as direct electron transfer hydrogen peroxide transducers for glucose biosensors, after coupling to GOx. Both HRP/GOx–PAP and HRP/GOx–PAP SAM biosensors were prepared and fully characterized from an analytical point of view.

3.1. Determination of diffusion coefficient across PAP layer

We used the approach based on chronoamperometry (CA) and the Cottrell equation to determine the influence of the PAP layer on the diffusion of the following redox mediators: 2-2′-azino-bis(3-ethylbenzothiazoline-6-sulfonic acid) diammonium salt (ABTS), potassium ferrocyanide (FCN), ferrocene monocarboxylic acid (FCA).

The experimental results obtained in the determination of the diffusion coefficients of these substrates using a platinum microdisk, with (D_{PAP} in cm^2/s) and without PAP membrane (D_{sol} in cm^2/s), were the following: ABTS: $D_{sol} = (2.0 \pm 0.2) \times 10^{-6}$, $D_{PAP} = (3.2 \pm 0.2) \times 10^{-7}$; FCA: $D_{sol} = (4.6 \pm 0.4) \times 10^{-6}$, $D_{PAP} = (2.7 \pm 0.3) \times 10^{-6}$, FCN: $D_{sol} = (7.3 \pm 0.4) \times 10^{-6}$, $D_{PAP} = (1.2 \pm 0.1) \times 10^{-6}$ (data are the mean values of at least 10 determinations; R.S.D. is in the range 4–5%).

Even if D values in the presence of PAP are significantly smaller, the excellent diffusion properties exhibited by the PAP layer on the electrode surface for each electroactive species investigated are emphasized, in particular if compared to analogous works employing different membranes (Yin et al., 2007; Crumbliss et al., 1992). The results, indicating the good permeability of the PAP layer to classical electrochemical mediators, are of great importance in view of the use of PAP as immobilizing agent in second-generation biosensor development. It is deemed possible to account for the behavior of the diffusion coefficients for the compounds considered by examining the experimental data. Furthermore, it must be borne in mind that too few data are available to develop a convincing theory, since only three mediators have been considered. In any case, a certain number of considerations are possible, mainly based on the molecular structures: ABTS, being the bigger molecule, is more strongly affected by the PAP layer hindering the diffusion. A very similar reduction is observed for FCN, which is characterized by the presence of three charges in its structure; this could be explained in terms of possible electrostatic interactions with charges present in the PAP polymeric structure. Conversely, the diffusion coefficient of FCA (smaller and with only one charge) remains almost stable both with and without PAP coverage. In particular, FCA can be considered the most promising mediator as it can easily permeate a PAP layer and generate an electrochemical response.

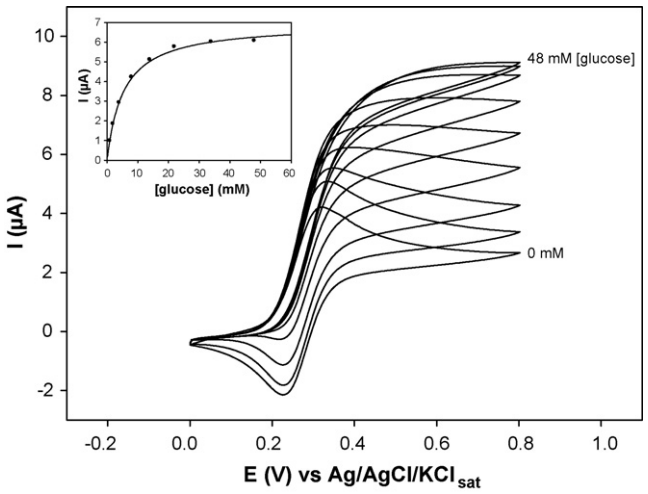

Fig. 1. Cyclic voltammograms of GOx–PAP immobilized on GCE, carried out in PB at 5 mV/s in presence of 1 mM FCA containing different concentrations of glucose; in the inset, the limiting current vs. glucose concentration is reported.

3.2. GOx–PAP-mediated biosensor

Having established its good permeability to different mediators, PAP was tested as enzyme immobilizing agent-support in the preparation of second-generation biosensors. To this end, glucose oxidase (GOx) was immobilized in the PAP layer on a GCE; the response of the resulting biosensor to increasing concentration of glucose (as substrate) was studied in 1 mM FCA solution (as mediator). This concentration value fits the requirement discussed elsewhere, namely that above a certain concentration value of reduced mediator, the catalytic current attains a limiting value, thus simplifying kinetic treatment and enabling an easy calculation of the parameters involved (Delle Noci et al., 2008).

In Fig. 1, the cyclic voltammograms obtained for different glucose concentrations are reported; the limiting current vs. glucose concentration displayed in the figure inset shows a Michaelis–Menten behavior. The use of a non-linear fitting

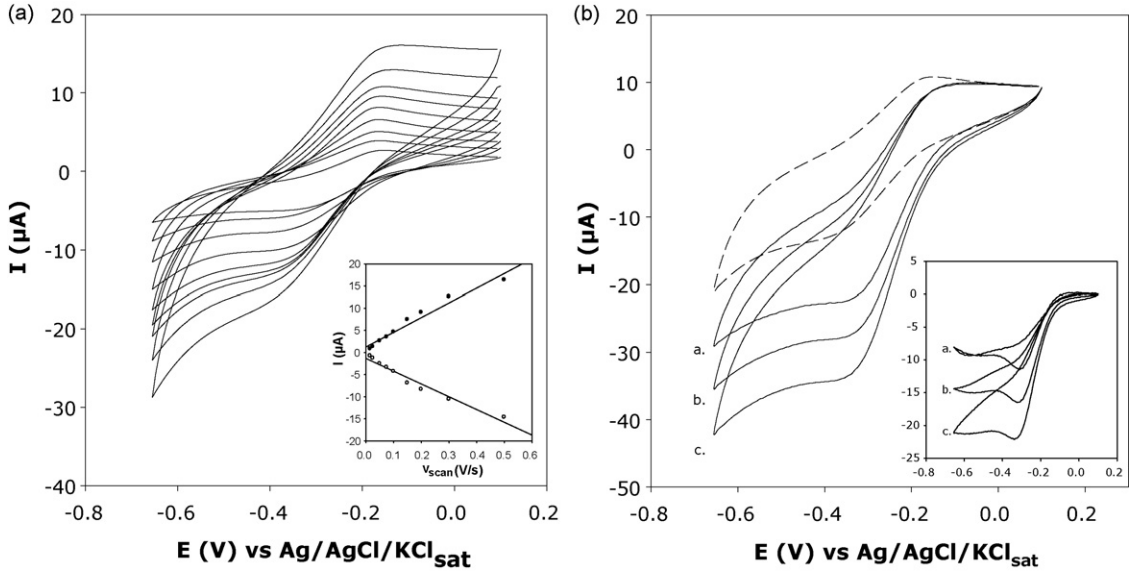

Fig. 2. Cyclic voltammograms of HRP–PAP immobilized on GCE in 0.1 M PB (pH 6.5): (a) carried out at different scan rates (from 15 to 500 mV/s); in the inset, the anodic and cathodic peak currents vs. scan rate is reported; (b) carried out at 200 mV/s scan rate, in presence of (a.) 0.4, (b.) 0.8 and (c.) 1.2 mmol/L H_2O_2 (dashed line refers to blank); in the inset, the signals obtained after blank subtraction is shown.

(SigmaPlot Kinetic Module, see http://www.sigmaplot.com) to these data allowed the main kinetic parameters to be computed; in particular, $K_{MS}^{app} = 5.4$ mM; $I_{max} = 7.05$ μA (correlation coefficient $r^2 = 0.9960$). The higher value of the immobilized GOx Michaelis constant than that obtained with the same enzyme free in solution (Delle Noci et al., 2008) confirms that the affinity towards a substrate of an enzyme is lowered, once the enzyme has been immobilized, as previously reported (Hong et al., 2007).

In order to evaluate the effect of enzyme concentration on analytical performance, several glucose biosensors characterized by different amounts of immobilized GOx were prepared. As expected, I_{max} decreases with time, indicating that the enzyme is both chemically and physically immobilized by PAP, as the physically entrapped fraction of the enzyme is more easily released into the measuring solution. Moreover, this is much more evident when GOx concentration is higher since the physically entrapped fraction becomes greater while the chemically immobilized one remains almost constant due to the limited number of reacting moieties in the PAP prepolymer.

In addition, the I_{max} varies linearly as the amount of enzyme increases in the range 5–30 μM. For higher GOx concentrations, the I_{max} value attains a plateau, and when GOx concentration exceeds 60 μM, a small decrease is observed. In fact, for low enzyme loading, the current response is limited by enzyme kinetics and I_{max} increases linearly with enzyme amount. The absence of any further increase in current response with additional enzyme amounts above 30 μM indicates that the transition from the enzyme's kinetics to the diffusion limit of the mediator has occurred. On the other hand, the higher enzyme concentration leads to an increased diffusion resistance against the enzymatically reduced mediator reaching the electrode surface, thus contributing to the observed decrease in maximum current. (Jin et al., 1995).

3.3. HRP-modified electrode: electron transfer characterization

3.3.1. HRP–PAP-modified electrode

Investigation by cyclic voltammetry on GCE (Fig. 2a) and SPE modified working electrodes displays a couple of quasi-reversible peaks. Using GCE the anodic and cathodic peaks are symmetric with an i_{pa}/i_{pc} ratio close to one; the peak current varies linearly with scan rate (see inset in Fig. 2a) as would be expected from an immobilized system not controlled by diffusion (Bard and Faulkner, 2002). Peak separation is $\Delta E_p = 140$ mV while the calculated redox formal potential is −370 mV vs. Ag/AgCl/KCl_{sat}, in good agreement with the redox potential value of HRP determined in solution by potentiometric titration (Harbury, 1959).

The ΔE_p value obtained was used to evaluate the electron transfer kinetic constant between electrode and enzyme using the Laviron method (Laviron, 1979); since $\Delta E_p < 200$ mV, the electrochemical transfer coefficient (α) can be approximated to $\alpha = 0.5$ with an error of less than 5% and the apparent electron transfer constant k_s can be evaluated by the well know Laviron's formulism.

The constant k_s was determined in the range 15–75 mV/s by considering a single exchanged electron, obtaining $k_s = 20\ s^{-1}$ for GCE and $k_s = 24\ s^{-1}$ for SPE, respectively. k_s was observed to increase with increasing scan rate. Surface coverage of electroactive peroxidase (Γ^*) was calculated using Faraday's law ($\Gamma^* = Q/nFA$; where Q is the exchanged charge and A the electrode surface) after anodic peak integration (Q). The results obtained are summarized in Table 1.

3.3.2. HRP–PAP SAM-modified electrode

Thanks to the special features of PAP, an immobilization method comprising self-assembled monolayers of different molecules was also tested. To this end, the HRP–PAP mixture was deposited onto

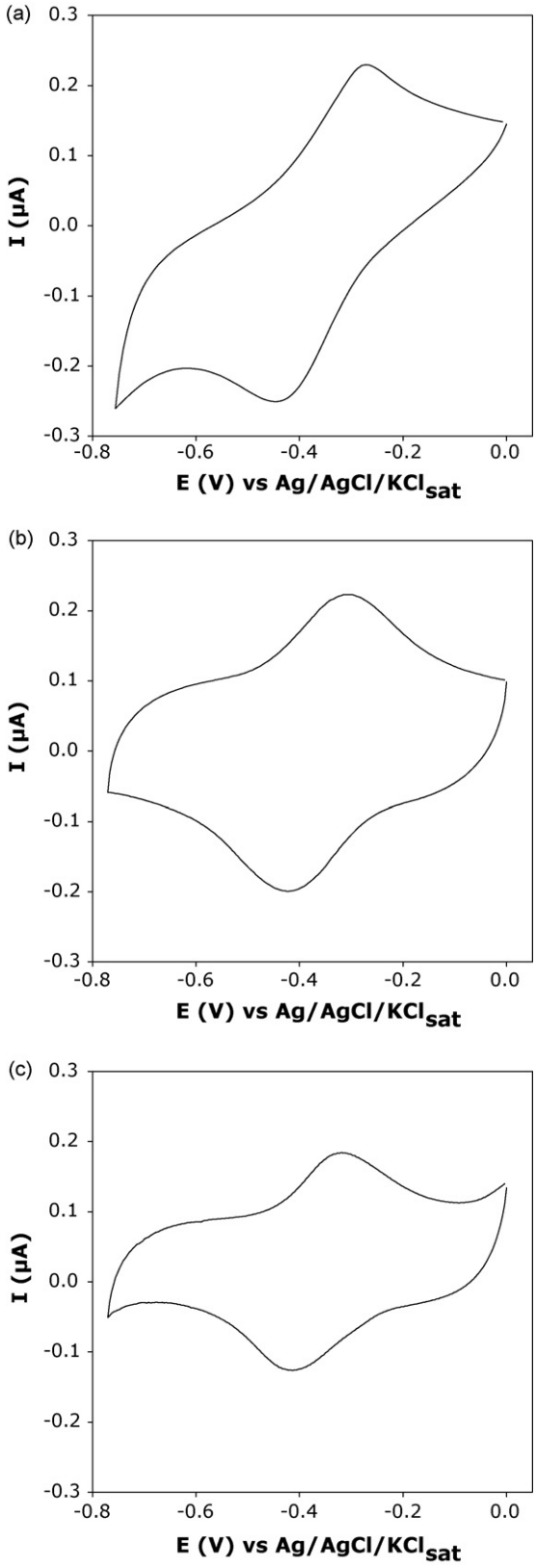

Fig. 3. Cyclic voltammograms of HRP–PAP immobilized on (a) GCE and different SAM covered electrodes: (b) MPA–AuE and (c) NTP–AuE, carried out in 0.1 M PB at pH 6.5 (scan rate 25 mV/s).

Table 1
Electrochemical parameters for HRP–PAP biosensors compared to those obtained for HRP–PAP SAM-based biosensors

Electrodes type	E^0 vs. Ag/AgCl (mV)	k_s (s^{-1})	Deposited HRP (mol/cm^2)	Electroactive HRP (Γ^*) (mol/cm^2)	% Electroactive protein
GCE	−370 ± 4	20	1.6×10^{-9}	$1.3 \pm 0.2 \times 10^{-11}$	0.81
SPE	−364 ± 5	24	8.0×10^{-9}	$2.0 \pm 0.4 \times 10^{-11}$	0.25
MPA–AuE	−376 ± 5	54	1.6×10^{-9}	$1.5 \pm 0.4 \times 10^{-11}$	0.94
NTP–AuE	−378 ± 3	76	1.6×10^{-9}	$1.8 \pm 0.1 \times 10^{-11}$	1.10

Measurements were carried out in PB 0.1 M (pH 6.5) and they are the mean values of at least 10 determinations.

Au electrode surfaces (AuE) covered by SAM of mercaptopropionic acid or 4-aminothiophenol (NTP), alternatively, in view of the fact that – as already mentioned – PAP is able to cross link both with carboxylic and amino groups.

Obtained results are reported in Fig. 3 indicating that once PAP-immobilized onto SAM–AuE, the HRP displays a better defined signal and a faster electron transfer rate if compared to what is obtained using GCE.

When NTP–SAM is employed, a more reversible signal is observed: the electron transfer rate, as indicated by the k_s value (see Table 1), is also increased (76 s^{-1} vs. 54 s^{-1} for MPA–SAM and 20 s^{-1} for GCE). The formal potential for MPA–AuE and NTP–AuE is very close and it is also slightly higher and closer to the formal potential of HRP in solution (Harbury, 1959) with respect to the value obtained using GCE. This is probably due to a better orientation of the enzyme on the electrode surface which enables a faster electron transfer and a more reversible electrochemical behavior. In addition, the observed kinetic constant of electron transfer is higher when NTP instead of MPA is employed; the difference can be explained by taking into account the presence of the aromatic ring (in NTP) which facilitates the electric contact with the surface while the aliphatic chain (in MPA) involves an electron tunneling event. Also the amount of electroactive protein is increased probably thanks to a closer contact with the surface ensured by the large amount of active moieties characterizing the SAM and suitable for PAP reactions with respect to the bare GCE surface.

3.4. Hydrogen peroxide detection: HRP-based biosensors characterization

3.4.1. HRP–PAP biosensor

Catalytic activity of immobilized HRP was evaluated on the basis of the response of the different enzymatic sensors after several additions of H_2O_2 to the measuring solution. No peak was observed at the PAP electrode in the presence of H_2O_2 in the potential range of 0 to −0.8 V, suggesting the PAP electrode was inactive to direct electron reduction of H_2O_2. However, at the HRP–PAP electrode, the reduction peak current was greatly enhanced in the presence of H_2O_2, corresponding to the decrease in the oxidation peak current and suggesting a typical electrocatalytic reduction process of H_2O_2. The reduction peak current increased with H_2O_2 concentration in solution (Fig. 2b). The catalytic H_2O_2 reduction current, measured considering the peak centered at −300 mV, was reported as a function of H_2O_2 concentration in a Lineweaver–Burk plot, thus allowing the calculation of the main kinetic parameters. The apparent Michaelis–Menten constant values (K_M^{app}) determined for immobilized HRP on both GCE and SPE are reported in Table 2 and are in good agreement with those reported in literature (Ferri et al., 1998; Xiao et al., 2000). In the same table, the main analytical parameters for the calibration curves to H_2O_2 are also summarized. The good sensitivity, the wide linear range, the interesting detection limit values encourage the use of both enzymatic electrodes as hydrogen peroxide transducers in biosensor preparation.

3.4.2. HRP–PAP SAM biosensors

The HRP–PAP SAM enzymatic sensors obtained were tested for their electrocatalytic properties using H_2O_2 as substrate, as previously done for HRP–PAP sensors based on 'bare' electrodes. The results obtained for the electrocatalytic characterization are reported in Table 2. Comparison of the results highlights the fact that when a SAM covered electrode is used, better overall analytical performances are obtained. When compared to the one using GCE, the SAM-based sensors display a wider linear range (between 2 and 3 decades), an almost 50% higher sensitivity, a lower limit of detection and even a smaller value of the Michaelis constant, thus indicating a stronger affinity for the substrate (see Table 2).

The lifetime of the HRP–PAP SAM-based biosensor expressed as a percentage of its original response was evaluated against a 0.1 mM H_2O_2 standard solution. During this period the biosensor was routinely used for 10–12 determinations per day; the biosensor, when not used, was stored in PBS at 4 °C. The decrease in the biosensor response was about 15–20% after 10 days, while its response decreased below 40–50% after 30 days operation.

3.5. Glucose detection: HRP/GOx-based biosensors characterization

3.5.1. HRP/GOx–PAP biosensors

Glucose biosensors were prepared by coupling the enzyme glucose oxidase (GOx) to the described HRP sensors as hydrogen peroxide transducer; to this end, an appropriate amount of GOx was added to the HRP–PAP mixture to be deposited on the electrode surfaces: both for HRP–GCE sensors, and for HRP–SPE sensors a 1:1 HRP:GOx ratio was employed. Measurements were carried out in PB in the presence of O_2 using glucose as substrate; the main analytical results are reported in Table 3. All the prepared glucose biosensors show good performance: a linearity range of approximately 2 decades, a limit of detection in the range of 10^{-4}–10^{-5} M and a good sensitivity.

Table 2
Kinetic and analytical parameters for HRP–PAP biosensors, H_2O_2 as substrate compared to those obtained for HRP–PAP SAM-based biosensors

Electrodes type	Linearity range (mM)	Sensitivity (μA/mM)	R.S.D. (%)	K_M (mM)	LOD (mM)	r^2
GCE	0.01–1.0	26.2 ± 0.7	2.0	4.3	3.0×10^{-3}	0.9981
SPE	0.03–0.80	19.3 ± 0.4	2.6	3.6	9.0×10^{-3}	0.9991
MPA–AuE	0.0050–1.40	33 ± 1	1.1	1.4	1.5×10^{-3}	0.9932
NTP–AuE	0.0006–1.50	37 ± 2	1.5	1.0	0.2×10^{-3}	0.9995

Measurements were carried out in PB 0.1 M (pH 6.5) and they are the mean values of at least 10 determinations.

Table 3
Analytical parameters for HRP/GOx–PAP and HRP/GOx–PAP SAM-based biosensors, glucose as substrate

Electrodes type	Linearity range (mM)	Sensitivity (μA/mM)	R.S.D. (%)	LOD (mM)	r^2
GCE	0.18–12	1.02 ± 0.04	3.9	0.06	0.9931
SPE	0.30–9.0	0.43 ± 0.02	2.9	0.10	0.9918
MPA–AuE	0.120–15.4	1.38 ± 0.09	4.0	0.04	0.9899
NTP–AuE	0.021–16.0	1.4 ± 0.1	3.8	0.007	0.9914

Measurements were carried out in PB 0.1 M (pH 6.5) and they are the mean values of at least 10 determinations.

3.5.2. HRP/GOx–PAP SAM biosensors

The HRP–PAP SAM enzymatic sensors obtained were employed as H_2O_2 transducers in the construction of glucose biosensors, as previously done for HRP–PAP sensors based on 'bare' electrodes. The results obtained for the biosensor characterization are reported in Table 3. Comparison of the results highlights the fact that when a SAM covered electrode is used, better overall analytical performances are obtained.

When SAM-based biosensors are used for glucose biosensor assembly an increase of performances is observed, in this case there is a much more contained improvement with respect to GCE-based one (Table 3). This may be considered confirmation that GOx kinetics is the rate determining the biosensor performance which thus cannot benefit from the huge improvement in hydrogen peroxide determination obtainable with SAM-based sensors. The stability of the HRP–PAP SAM electrode was also investigated. The lifetime of the biosensor performance expressed as a percentage of its original response was evaluated on a 5 mM glucose standard solution in the same conditions described for HRP–PAP biosensor. The decrease in biosensor response was about 20% after 10 days, while its response decreased below 40% after 30 days operation. These results point to a good long-term stability of the HRP/GOx–PAP SAM biosensor which may be accounted for in terms of the favorable micro-environment for the immobilized HRP and GOx possibly provided by the biocompatible PAP together with SAM.

4. Conclusion

The results indicate the suitability of PAP as an enzyme immobilizing agent for the development of both second- and third-generation biosensors; specifically (i) a good permeability of the PAP layer to classical electrochemical mediators; (ii) the efficient entrapment of proteins therein without loss of bioelectrochemical properties, suggesting instead the maintenance of the native-like structural properties and (iii) the effective heterogeneous electron transfer at the interface PAP-electrode surface have been demonstrated.

Moreover, the use of PAP resulted in a simplified and cost-effective immobilization procedure that also ensured a good stability and reproducibility of the enzymatic–polymeric film. When used as immobilizing agent, PAP offers a biocompatible micro-environment for confining biomacromolecules and foreshadows the great potentiality of this immobilizing agent not only in theoretical studies of protein direct electron transfer but also from an applications point of view, in the development of second- and third-generation biosensors as is fully demonstrated in this paper.

Acknowledgements

This work was carried out with the financial support of the University of Rome "La Sapienza" and of the European Commission under contract number 017350 (BioMedNano).

References

Adams, R.N., 1969. Electrochemistry at Solid Electrodes. Marcel Dekker, New York.
Armstrong, F.A., Wilson, G.S., 2000. Electrochim. Acta 45, 2623–2645.
Bard, A.J., Faulkner, L.R., 2002. Electrochem. Methods, 2nd edition. Wiley, New York.
Botrè, C., Botrè, F., Galli, M., Lorenti, G., Mazzei, F., Porcelli, F., 1992. Anal. Biochem. 201 (2), 227–232.
Crumbliss, A.L., Perine, S.C., Edwards, A.K., Rillema, D.P., 1992. J. Phys. Chem. B 96, 1388–1394.
De Groot, M.T., Merkx, M., Koper, T.M., 2005. J. Am. Chem. Soc. 127, 16224–16232.
De Groot, M.T., Evers, T.H., Merkx, M., Koper, T.M., 2007. Langmuir 23, 729–736.
Delle Noci, S., Frasconi, M., Favero, G., Tosi, M., Ferri, T., Mazzei, F., 2008. Electroanalysis 20, 163–169.
Denuault, G., Mirkin, M.V., Bard, A.J., 1991. J. Electroanal. Chem. 308, 27–38.
Ferri, T., Poscia, A., Santucci, R., 1998. Bioelectrochem. Bioeneg. 45, 221–226.
Gorton, L., Lindgren, A., Larsson, T., Munteanu, F.D., Ruzgas, T., Gazaryan, I., 1999. Anal. Chim. Acta 400, 91–108.
Harbury, H.A., 1959. J. Biol. Chem. 225, 1009–1017.
Hong, J., Moosavi-Movahedi, A.A., Ghourchian, H., Rad, A.M., Rezaei-Zarchi, S., 2007. Electrochim. Acta 52, 6261–6267.
Jin, W., Bier, F., Wollenberger, U., Scheller, F., 1995. Biosens. Bioelectron. 10, 823–829.
Katz, E., Willner, I., 2004. Angew. Chem. Int. Ed. 43, 6042–6108.
Laviron, E.J., 1979. J. Electroanal. Chem. 101, 19–28.
Lu, X., Wen, Z., Li, J., 2006. Biomaterials 27, 5740–5747.
Lu, Q., Hu, C., Cui, R., Hu, S., 2007. J. Phys. Chem. B 111, 9808–9813.
Mascini, M., Mazzei, F., 1987. Anal. Chim. Acta 192 (1), 9–16.
Mazzei, F., Botrè, F., Lorenti, G., Porcelli, F., 1996. Anal. Chim. Acta 328 (1), 41–46.
Mazzei, F., Botrè, F., Montilla, S., Pilloton, R., Podestà, E., Botrè, C., 2004. J. Electroanal. Chem. 574 (1), 95–100.
Petrovic, S.C., Zhang, W., Ciszkowska, M., 2000. Anal. Chem. 72, 3449–3458.
Shan, D., Han, E., Xue, H., Cosnier, S., 2007. Biomacromolecules 8, 3041–3046.
Wang, J., 2008. Chem. Rev. 108, 814–825.
Wang, J., Musameh, M., Lin, Y., 2003. J. Am. Chem. Soc. 125, 2408–2409.
Xiao, Y., Ju, H.X., Chen, H.Y., 2000. Anal. Biochem. 278, 22–29.
Yin, Y., Zhang, H., Nishinari, K., 2007. J. Phys. Chem. B 111, 1590–1596.
Zhang, M., Smith, A., Gorski, W., 2004. Anal. Chem. 76, 5045–5050.
Zhang, Q., Zhang, L., Liu, X., Li, J., 2007. Biosens. Bioelectron. 23, 695–700.
Zhuo, Y., Yuan, R., Chai, Y.Q., Sun, A.L., Zhang, Y., Yang, J.Z., 2006. Biomaterials 27, 5420–5429.